

# Anion of Tetrachloroethane (Tetra): Fragmentation and Geminate Ion Kinetics in Liquid Methylcyclohexane (MCH)

Rolf E. Bühler\* and Murat A. Quadir†

Laboratory for Physical Chemistry, ETH Zürich, Switzerland

Received: April 18, 2003; In Final Form: September 29, 2003

In the context of studies on the influence of the anion lifetime on the geminate ion kinetics, 1,1,1,2- and 1,1,2,2-tetrachloroethane (1112-Tetra and 1122-Tetra) were studied as solutes in liquid methylcyclohexane (MCH) at low temperatures (133–183 K). The two isomers serve as examples of long anion lifetime. The analysis of the pulse radiolysis data was based on the  $t^{-0.6}$  semiempirical law for geminate ion kinetics. The visible band with  $\lambda_{\text{max}} = 450$  or 430 nm is shown to be due to the anion of 1112-Tetra or 1122-Tetra, respectively. Its kinetics relates to three consecutive geminate pairs of ions, due to two ionic reactions: (a) *The fast process* represents the cationic mechanism: the precursor cation  $M^{+*}$  relaxes (or isomerizes) to the high mobility ion  $MCH^+$  ( $k_r$ ) and simultaneously fragments ( $k_f$ ) to a diffusional methylcyclohexene<sup>+</sup> ( $MCHene^+$ ). The total  $M^{+*}$  decay ( $k_{\text{tot}} = k_r + k_f$ ) produces mixed cations ( $MCH^+, MCHene^+$ ). (b) *The slow process* is due to the anion fragmentation ( $k^-$ ) from  $Tetra^-$  to  $Cl^- + R^*$ , with  $\tau^- = 13.7$  or  $20.0 \mu\text{s}$  (143 K) for 1112- or 1122-Tetra, respectively. The fragment radical  $R^*$  is freed too late to allow scavenging of positive charge. *The three geminate pairs of ions* are ( $M^{+*}/Tetra^-$ ), ( $MCH^+, MCHene^+/Tetra^-$ ), and ( $MCH^+, MCHene^+/Cl^-$ ). All ions (except  $Cl^-$ ) contribute to the optical absorption. The *rate constants*  $k_{\text{tot}}$  and  $k^-$  are both independent of the concentration of Tetra. For  $k_{\text{tot}}$  this means that  $M^{+*}$  decays in a fixed ratio of  $k_f$  to  $k_r$ . This is in contrast to previous findings with  $N_2O$  or  $CHCl_3$  but corresponds to our recent proposal that  $M^{+*}$  appears to represent some isomer of  $MCH^+$  in a higher energy state (or of higher ionization potential). The *anion fragmentation rate* for 1112-Tetra is  $k^-(143 \text{ K}) = (7.3 \pm 0.6) \times 10^4 \text{ s}^{-1}$  with  $E_{\text{act}} = 17.8 \text{ kJ/mol}$  and  $\log A = 11.2$ . For 1122-Tetra it is  $k^-(143 \text{ K}) = (5.0 \pm 1.0) \times 10^4 \text{ s}^{-1}$  with  $E_{\text{act}} = 16.9 \text{ kJ/mol}$  and  $\log A = 10.9$ . The *free ion intercepts*, from the  $t^{-0.6}$ -simulations, reveal for all geminate pairs with  $Tetra^-$  a strong dependence on the Tetra concentration  $[T]$ , even though complete electron scavenging was ascertained. This is explained by the formation of dimer anions  $T_2^-$  through an equilibrium  $T^- + T \rightleftharpoons T_2^-$ . The absorption at 450 nm (or 430 nm) then is due to  $T_2^-$  (most likely a charge resonance transition ( $T \leftarrow T^-$ )). For the initial geminate pair ( $M^{+*}/Tetra^-$ ), the free ion intercept was smaller than the one for  $Tetra^-$  alone (actually  $T_2^-$ ). As this result was based on the assumption that  $M^{+*}$  and  $MCH^+$  have the same mobility, this now reveals that the precursor cation  $M^{+*}$  must have at least a 9 times higher mobility than  $MCH^+$ .

## I. Introduction

In the adjacent paper<sup>1</sup> (and its preceding one<sup>2</sup>) the effect of the anion lifetime on the geminate ion kinetics is discussed for chlorocarbons in liquid methylcyclohexane (MCH). In the context of that paper, tetrachloroethane (Tetra) served as an example of long anion lifetime. Its results yet revealed additional insights into the behavior of cations and anions in general, far beyond the effect of anion lifetime on geminate ion kinetics. Therefore, the results for tetrachloroethane are discussed in this separate paper. From the analysis of the geminate ion kinetics for tetrachloroethane, it has been concluded that the mobility of the cationic precursor  $M^{+*}$  must be higher than the one of  $MCH^+$ —not the same, as was previously assumed. Furthermore, to explain the concentration dependences of the free ion intercepts,

the formation of dimer anions through the equilibrium  $Tetra^- + Tetra \rightleftharpoons Tetra_2^-$  is proposed. Details follow in this paper.

## II. Experimental Section

**A. Methods.** The technique of pulse radiolysis with a Febetron 705 accelerator (Physics International) for 30 ns pulses of 2 MeV electrons has been used as reported in the adjacent paper.<sup>1</sup> Experiments with methylcyclohexane (MCH) as solvent were typically performed in the temperature range from 133 to 183 K in the liquid state. A typical dose was between 50 and 120 Gy. All data usually are normalized to 100 Gy. All the experimental signals were corrected for the cell window signal (quartz defects).<sup>3</sup> The origin of shock waves in pulse radiolysis cells and the method to minimize the effect have also previously been discussed in detail.<sup>3,4</sup>

**B. Chemicals.** Methylcyclohexane (MCH) (Fluka purum, >98% GC) was passed through a column of aluminum oxide, dried over molecular sieves A4, and then fractionated through a Fischer “Spaltrohrkolonne” with about 30 theoretical plates. 1,1,1,2-Tetrachloroethane (1112-Tetra,  $CCl_3CH_2Cl$ ) and 1,1,2,2-

\* To whom correspondence should be addressed. Mailing address: Physical Chemistry, ETH Zürich, Mühlebachstrasse 96, 8008 Zürich, Switzerland. Telephone: +41-1-383 16 13. Fax: +41-1-383 06 88. E-mail: buehler@phys.chem.ethz.ch.

† Present address: L’Oreal USA, Applied Research, 285 Terminal Ave., Clark, NJ 07066, USA.

tetrachloroethane (1122-Tetra,  $\text{CHCl}_2\text{CHCl}_2$ ) from Aldrich (>99%) and  $\text{N}_2\text{O}$  from PanGas, Luzerne CH (99%), were used as received.

### III. Method of Data Analysis

The simulation of the rate data is described in detail in the adjacent paper.<sup>1</sup> The basis is the semiempirical  $t^{-0.6}$  kinetic law for the geminate ion recombination, as initiated by van den Ende et al.<sup>5</sup> It describes the probability of survival of the geminately recombining ions relative to the free ion yield:

$$\frac{G(t)}{G_{\text{fi}}} = 1 + \alpha t^{-0.6} = \frac{\text{absorbance}(t)}{\text{absorbance}(\infty)} = \frac{A(t)}{IA}$$

$$\text{with } \alpha = 0.6 \left[ \frac{r_c^2}{D} \right]^{0.6} \quad (1)$$

where  $\alpha$  is the mobility value and  $IA = A(\infty)$  is the free ion intercept.

Any plot of the absorbance  $A(t)$  against  $t^{-0.6}$  should be linear. Its intercept  $IA$  for  $t = \infty$  ( $t^{-0.6} = 0$ ) corresponds to the absorbance of the free ion yield. The slope divided by the intercept  $IA$  is called  $\alpha$ , a mobility value (or  $\beta$ ,  $\gamma$ , etc. for other geminate pairs). From this value, with the known Onsager radius  $r_c$ , an experimental diffusion constant can be derived:  $D_{\text{exp}} = D^+ + D^-$ .

Theoretical support for the  $t^{-0.6}$  rate law was given by Bartczak and Hummel.<sup>6,7</sup> We have given experimental support<sup>2,3,8-13</sup> and could derive some experience about the validity range: for low-temperature studies in liquid MCH (e.g. 143 K) the  $t^{-0.6}$  kinetic law holds at least to  $t^{-0.6} = 4.0$  ( $t \geq 100$  ns). In this range all deviations from the  $t^{-0.6}$  linearity had a chemical reason and could be explained.

For this purpose the theory was extended to cover ionic reactions, which are overlapping with the geminate ion recombination kinetics. It also covers combinations of ionic reactions (parallel or consecutive, for positive and/or negative ions) and is able to simulate ion recombinations leading to products, which are optical absorbers. In this paper the mathematical equations needed are quoted from the adjacent paper,<sup>1</sup> referring to eqs 1–12.

### IV. Results

In MCH solutions the initial process usually corresponds to the mechanism of the high mobility cations: with the precursor cation  $\text{M}^{+\ast}$  relaxing (or isomerizing) into the high mobility radical cation  $\text{MCH}^+$  ( $k_r$ ) and, in parallel, fragmenting ( $k_f$ ) into the diffusional cation of methylcyclohexene ( $\text{MCHene}^+$ ).<sup>3,8,9,11-13</sup> The solvated electron is scavenged by the solute Tetra (T) to form its anion Tetra<sup>-</sup> (or  $\text{T}^-$ ), which is expected to have a long fragmentation lifetime.<sup>1</sup> The solute Tetra might also influence the relative yields of  $\text{MCH}^+$  and  $\text{MCHene}^+$ . Scheme 1 represents the expected mechanism, where  $k_r = k_0 + k_2[\text{T}]$  includes a possible concentration dependence. It corresponds to the finding with chloroform as solute.<sup>8</sup> To test Scheme 1, the chemical systems of Table 1 were studied in detail with both isomers.

All observations and discussions will be limited to the time range after completion of electron scavenging by Tetra, taken as 99% scavenged (anchor point<sup>14</sup> for  $\text{e}_{\text{solv}}^- + \text{T}$ ). A rate constant  $k_e$  for electron-scavenging was derived from the known diffusion constants at 143 K:  $D(\text{e}_{\text{solv}}^-) = 1.6 \times 10^{-6} \text{ cm}^2 \text{ s}^{-1}$  (ref 9) and  $D(\text{Tetra}) \approx D(\text{MCH}^+)_{\text{theor}} = 9.4 \times 10^{-9} \text{ cm}^2 \text{ s}^{-1}$  (the theoretical value for diffusional mobility of  $\text{MCH}^+$  (ref 3).

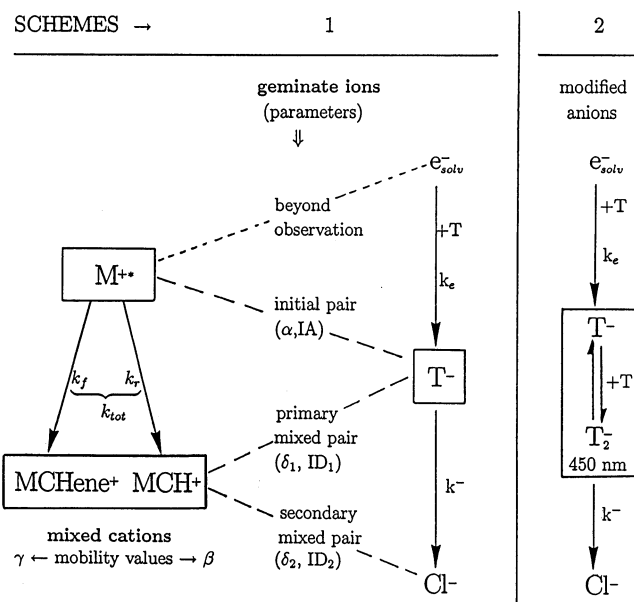


**TABLE 1: Chemical Systems Studied for the Two Isomers of Tetra in MCH**

system	concentration	temp/K	$\lambda/\text{nm}$	comments
1,1,1,2-Tetrachloroethane (1112-Tetra)				
A	5.3–530 mM	143	450, 570	conc variation
B	0.2 M	143	350–650	transient spectra
C	0.2 M	143	350–650	with $\text{N}_2\text{O}$ sat. (0.118 M)
D	0.2 M	133–163	450	temp variation
1,1,2,2-Tetrachloroethane (1122-Tetra)				
E	0.2 M	143	350–750	transient spectra
F	0.2 M	153	450	with $\text{N}_2\text{O}$ sat. (0.118 M)
G	0.2 M	143–183	450	temp variation

The reactant radii were chosen to be 0.2 or 0.3 nm for  $\text{e}_{\text{solv}}^-$  or Tetra, respectively. Therefore, the diffusional rate constant for electron scavenging at 143 K is  $k_e = 4.8 \times 10^8 \text{ M}^{-1} \text{ s}^{-1}$ . This then allows us to calculate the corresponding “anchor point” AP (ref 14) for the  $t^{-0.6}$  plots:  $\text{AP}_e(1\%) = 0.4 \times (k_e[\text{T}] \times 10^{-6})^{0.6}$ . For all concentrations  $[\text{Tetra}] \geq 90 \text{ mM}$  our complete experimental time window ( $t \geq 100 \text{ ns}$ , means  $t^{-0.6} \leq 4.0 \mu\text{s}^{-0.6}$ ) is unaffected by the scavenging process. For lower concentrations the observation window was reduced correspondingly.

**A. Initial Spectral Observations.** The transient spectra as shown in Figure 1 for both Tetra isomers uniformly decay over the band displayed. There is no  $\lambda_{\text{max}}$  shift with time, as found for other halocarbons (hexa- and pentachloroethane<sup>1</sup>). By saturating with  $\text{N}_2\text{O}$  the earliest transient spectrum is reduced by about 10%, without changing the decay rate (see below). It is therefore obvious that the bands with  $\lambda_{\text{max}}(1112\text{-Tetra}) = 450 \text{ nm}$  and  $\lambda_{\text{max}}(1122\text{-Tetra}) = 430 \text{ nm}$  must be due to the corresponding anion  $\text{T}^-$  with  $\text{e}_{\text{solv}}^-$  as their precursor.

**B. Initial Kinetic Observations.** A typical rate curve ( $t^{-0.6}$  plot) for 0.2 M 1112-Tetra in MCH at 143 K is shown in Figure 2. The general shape is similar to the one found for chloroform<sup>8</sup> in MCH. The early part (large  $t^{-0.6}$  values) again appears to correspond to the cationic mechanism ( $\text{M}^{+\ast} \rightarrow \text{MCH}^+$ ,  $\text{MCHene}^+$ ). The late part (small  $t^{-0.6}$  values) reveals that the anion decay is much slower than that for chloroform. Therefore, the positive (early) and negative (late) processes are better separated in time than in the system with  $\text{CHCl}_3$ .

**C. Initial Simulations.** As usual, simulation has to start at late times, with the slower process (anion fragmentation with  $k^-$ ) and then continue to early times ( $\text{M}^{+\ast}$  decay with  $k_{\text{tot}}$ ).

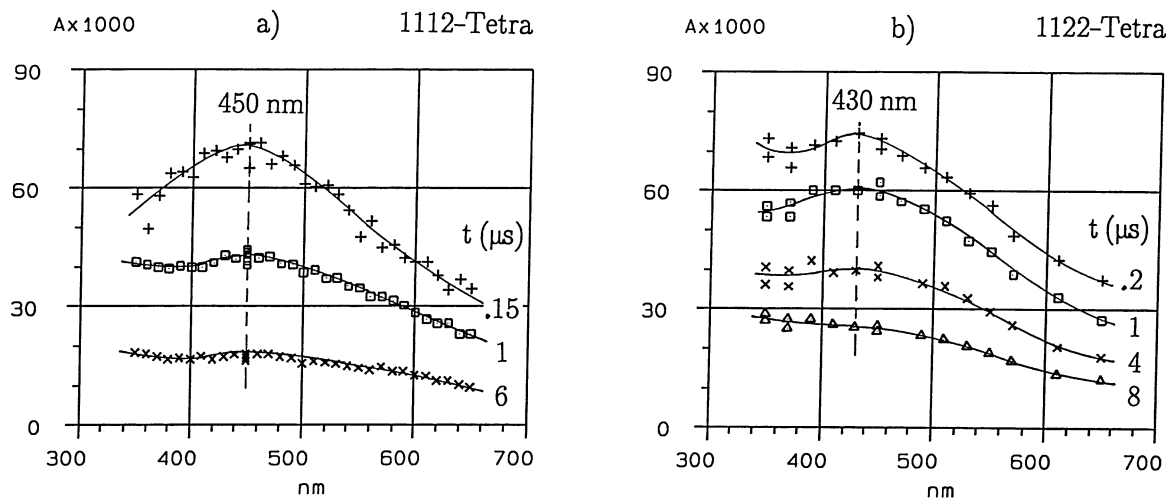


**Figure 1.** Transient spectra for the two isomers of Tetra in MCH at 143 K: (a) 0.2 M 1112-Tetra (bandwidth hwhm =  $6400 \pm 200 \text{ cm}^{-1}$ ) and (b) 0.2 M 1122-Tetra (bandwidth hwhm =  $7200 \pm 300 \text{ cm}^{-1}$ ). Absorbance  $A$  normalized to 100 Gy.

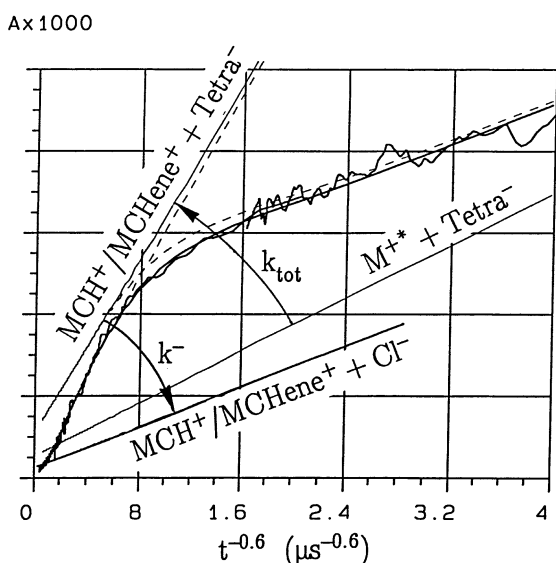


**Figure 2.**  $t^{-0.6}$  plot of a rate curve at 450 nm for a solution of 0.2 M 1112-Tetra in MCH at 143 K. Absorbance  $A$  normalized to 100 Gy. The simulation corresponds to Scheme 1 and is based on the following data: the initial geminate pair ( $M^{+*}/Tetra^{-}$ ) with  $\alpha = 3.0 \mu\text{s}^{0.6}$ ,  $IA = 4.3 \times 10^{-3}$ ; the primary mixed pair ( $MCH^+, MCHene^+/Tetra^-$ ) with  $\delta_{\text{mix}} = 5.0 \mu\text{s}^{0.6}$ ,  $ID_1 = 8.6 \times 10^{-3}$ ; the secondary mixed pair ( $MCH^+, MCHene^+/Cl^-$ ) with  $\delta_{\text{mix}} = 5.0 \mu\text{s}^{0.6}$ ,  $ID_2 = 2.0 \times 10^{-3}$ ; and the two rate constants  $k_{\text{tot}} = 1.6 \times 10^6 \text{ s}^{-1}$  and  $k^- = 7.0 \times 10^4 \text{ s}^{-1}$ .

The anion decay is so slow that the final  $t^{-0.6}$  linearity ( $\delta_2$ ,  $ID_2$ ) for the mixed geminate ions ( $MCH^+, MCHene^+/Cl^-$ ) is not available. If the  $\delta_2$  values are taken from the  $\text{CHCl}_3$  system,<sup>8</sup> then the resulting  $ID_2$  values are too low, from what is known from previous experiments.<sup>3,8,9,11</sup> The  $ID_2$  values (free ion yield) therefore were calculated from the known  $MCH^+$  and  $MCHene^+$  spectra<sup>8</sup> for the particular  $MCH^+/MCHene^+$  ratio (Figure 3). The  $\delta_2$  values from the  $\text{CHCl}_3$  system then were too large to simulate the systems with  $[T] < 0.1 \text{ M}$ .  $\delta_2$  was reduced until a complete fit for all concentrations (5.3–530 mM Tetra) was reached (see Final Simulation).

Simulation of the early times revealed a very small concentration dependence for  $k_{\text{tot}} = k_f + k_0 + k_2[T]$ . Within error limits,  $k_2$  appears to be near zero. In consequence, the  $\delta_2$  values should also be independent of  $[T]$ : there is no change of the ratio  $MCH^+/MCHene^+$  with  $[T]$ . The mobility value  $\delta_2$  only depends on  $\lambda$  due to  $\epsilon(MCH^+)$  and  $\epsilon(MCHene^+)$  (see eq 6 of ref 1).

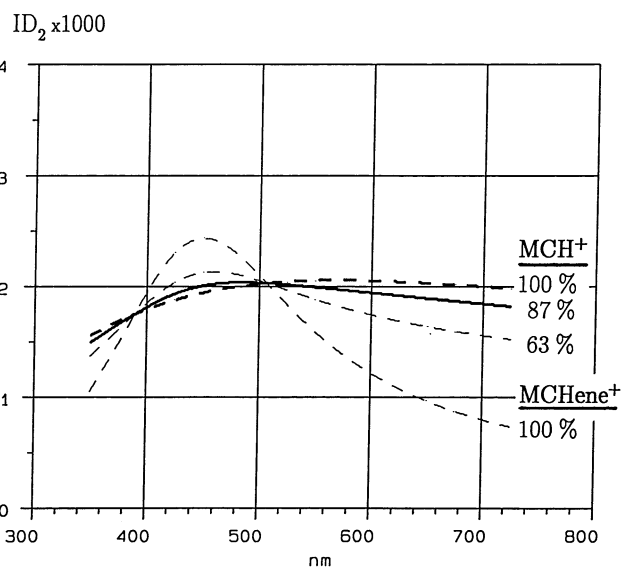


**Figure 3.** Calculated intercepts  $ID_2$  for selected ratios of  $MCH^+$  and  $MCHene^+$  from the known spectra of  $MCH^+$  and  $MCHene^+$  alone,<sup>8</sup> with  $G_{fi} = 0.06 (100 \text{ eV})^{-1}$ . The curves for 87% and 100%  $MCH^+$  correspond to  $\delta_{\text{mix}}$  and  $\delta_{\text{fast}}$ , respectively (see text). The curve for 63%  $MCH^+$  is from the  $\text{CHCl}_3$  system<sup>8</sup> for comparison.

**D. Final Simulations.** Several iterative cycles of simulations were necessary to reach the above initial conclusions, using all experiments from system A (Table 1) covering the concentrations  $5.3 \text{ mM} \leq [T] \leq 530 \text{ mM}$ . It was recognized that the rate constants  $k^-$  and  $k_{\text{tot}}$  varied rather little with the iteration cycles. The final experimental  $\delta_2$  value at 450 nm was  $\delta_2 = 5.0 \mu\text{s}^{0.6}$  (143 K). It corresponds to  $k_r/k_f = 6.6 (k_b/k_c)$  in eq 6 of ref 1). This ratio allows us to calculate the  $\lambda$  dependence of  $\delta_2$  (Figure 4) and corresponds to a composition of about 13%  $MCHene^+$  and 87%  $MCH^+$  for the mixed cations. These  $\delta_2$  values represent upper limits for complete simulation. They will be called  $\delta_{\text{mix}}$ . As  $\delta_1$  differs from  $\delta_2$  only by the mobility difference of the anion ( $T^-$  versus  $Cl^-$ ), which is negligible relative to the high mobility of the cation, it is equal to  $\delta_2$ , which means  $\delta_1 = \delta_2 = \delta_{\text{mix}}$ .

**Alternative Simulation.** For all data, the simulation is also possible with the lowest  $\delta_2$  value ( $\delta_2 = 3.0$  at 143 K) corresponding to 100%  $MCH^+$  yield (no  $M^{+*}$  fragmentation). This  $\delta_2$  represents the fastest process and will be called  $\delta_{\text{fast}}$ . So far there are no clear criteria to decide about the real  $\delta_2$

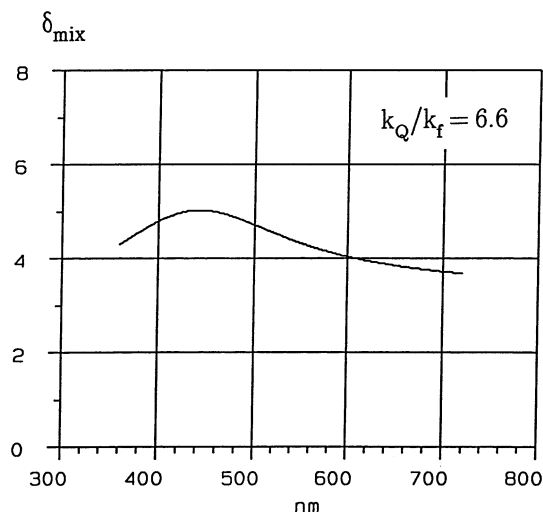


**Figure 4.**  $\lambda$  dependence of  $\delta_{\text{mix}}$  as calculated from eq 6 in ref 1. It is based on the experimental value  $\delta_{\text{mix}}(450 \text{ nm}) = 5.0 \mu\text{s}^{0.6}$ , which yields  $k_f/k_r = 6.6$ . The absorption coefficients of  $\text{MCH}^+$  and  $\text{MCHene}^+$ , and the mobility values  $\beta = 3.0 \mu\text{s}^{0.6}$  for  $\text{MCH}^+$  and  $\gamma = 15.7 \mu\text{s}^{0.6}$  for  $\text{MCHene}^+$  are used as published.<sup>8</sup>

**TABLE 2: Summary of the Rate Data at 143 K<sup>a</sup>**

system	$k^-/10^4$ $\text{s}^{-1}$	$k_{\text{tot}}/10^6$ $\text{s}^{-1}$
1112-Tetra in MCH		
A, conc variation	$(6.9 \pm 1.0)$	$(1.70 \pm 0.10)$
B, $\lambda$ variation	$(8.0 \pm 0.8)$	$(1.54 \pm 0.14)$
C, with $\text{N}_2\text{O}$ sat.	$(7.0 \pm 0.8)$	$(1.61 \pm 0.09)$
mean	$(7.3 \pm 0.6)$	$(1.60 \pm 0.10)^c$
1122-Tetra in MCH		
G, temp variation	$(5.0 \pm 1.0)$	$(1.35 \pm 0.20)$

<sup>a</sup> On the basis of  $\delta_{\text{mix}}$ . For the results with  $\delta_{\text{fast}}$ , see the Discussion, part C. <sup>b</sup>  $k_{\text{tot}} = k_f + k_0 + k_2[\text{T}]$ . <sup>c</sup> As  $k_{\text{tot}}$  is not dependent on  $[\text{T}]$ ,  $k_2 \approx 0$ . With  $\sim 13\%$   $\text{MCHene}^+$  (model with  $\delta_{\text{mix}}$ )  $k_f \approx 0.2 \times 10^6 \text{ s}^{-1}$  and  $k_0 \approx 1.4 \times 10^6 \text{ s}^{-1}$ .

between  $\delta_{\text{mix}}$  (maximum) and  $\delta_{\text{fast}}$  (minimum). All simulations have been done with both limiting values. However, if one looks back to all previous systems studied in MCH,<sup>8,9,11</sup> the fraction of  $\text{MCHene}^+$  has always been higher than the 13%. It is expected that the results with  $\delta_{\text{mix}}$  are the more likely ones. They are documented throughout in this paper. The kinetic results for  $\delta_{\text{fast}}$  differ little from the ones with  $\delta_{\text{mix}}$  and do not supply additional insights. For a comparison, see the Discussion, part C.

A typical simulation with  $\delta_{\text{mix}}$  for a rate curve at 450 nm is seen in Figure 2 for 0.2 M 1112-Tetra at 143 K, corresponding to Scheme 1. The parameters for the three geminate pairs of ions and the rate constants for  $k_{\text{tot}}$  and  $k^-$  are given in the caption of Figure 2. The  $\alpha$  value for the high mobility of  $\text{M}^{+*}$  was assumed to be identical to the one of  $\text{MCH}^+$ .<sup>9</sup> For a better value, see the Discussion, part B.

**E. Dependence on Concentration [T].** From the kinetic analysis of all rate curves of system A with 1112-Tetra (Table 1) the concentration dependences of the rate constants  $k_{\text{tot}}$  and  $k^-$  and the intercepts (IA,  $\text{ID}_1$ ) were derived with  $\delta_{\text{mix}}$  (Figure 4).

The rate constant  $k^-$  for the anion fragmentation is constant within experimental error for the complete concentration range from 5.3 to 530 mM Tetra. This mean value for system A is  $\bar{k}^- = (6.9 \pm 1.0) \times 10^4 \text{ s}^{-1}$  at 143 K (Table 2).

The rate constant  $k_{\text{tot}}$  is shown in Figure 5. Above the concentration of  $\sim 50$  mM Tetra,  $k_{\text{tot}}$  is about constant, which means that  $k_2$  must be near zero and  $k_f \approx k_0$ . Even if 0.2 M

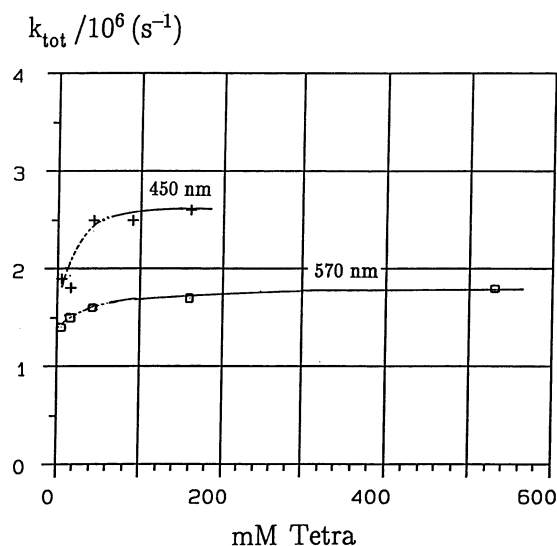


**Figure 5.** Concentration dependence of  $k_{\text{tot}} = k_f + k_r$  with  $k_r = k_0 + k_2[\text{T}]$  from the chemical system A (Table 1). For  $[\text{T}] \geq 50$  mM the rate constant  $k_{\text{tot}}$  levels off, which means  $k_2 \approx 0$  and  $k_f = k_0$ .

Tetra is saturated with  $\text{N}_2\text{O}$  (0.118 M), there is no further change of  $k_{\text{tot}}$  (see below: results with  $\text{N}_2\text{O}$ ). The initial increase at very low  $[\text{T}]$  most likely is not real, as the accuracy rapidly drops at low  $[\text{T}]$ .  $k_{\text{tot}}$  at 570 nm (versus 450 nm) is expected to be more reliable (less interference from the strong anion absorption) and furthermore corresponds to the results from systems B and C (see Table 2). For system A the mean value is  $\bar{k}_{\text{tot}}^- = (1.70 \pm 0.10) \times 10^6 \text{ s}^{-1}$ , almost independent of  $[\text{T}]$  (Table 2). As  $\delta_{\text{mix}}$  represents a yield of about 13%  $\text{MCHene}^+$ , the individual rate constants for fragmentation and relaxation (or isomerization) are  $k_f \approx 0.2 \times 10^6 \text{ s}^{-1}$  and  $k_r \approx 1.5 \times 10^6 \text{ s}^{-1}$ .

The free ion intercepts  $\text{IA}(\text{M}^{+*}/\text{Tetra}^-)$  and  $\text{ID}_1(\text{MCH}^+, \text{MCHene}^+/\text{Tetra}^-)$  are shown in Figure 6 (solid lines) as a function of  $[\text{T}]$ . The difference of  $\text{ID}_1(\text{MCH}^+, \text{MCHene}^+/\text{Tetra}^-)$  and  $\text{ID}_2(\text{MCH}^+, \text{MCHene}^+/\text{Cl}^-)$  corresponds to the absorption of  $\text{Tetra}^-$ , the expected free ion yield:  $\Delta\text{T}^- = \text{ID}_1 - \text{ID}_{2,\text{calc}}$  (Figure 6b, heavy lines). All free ion intercepts (IA,  $\text{ID}_1$ , and  $\Delta\text{T}^-$ ) are increasing with  $[\text{T}]$ . They should, however, be constant, as soon as all free ions are scavenged by Tetra. This condition is met in the whole concentration range studied. For an explanation, see the Discussion, part A.

**F. Free Ion Spectra.** From system B (Table 1) with 0.2 M 1112-Tetra at 143 K, the intercept spectra for  $\text{IA}(\text{M}^{+*}/\text{Tetra}^-)$ ,  $\text{ID}_1(\text{MCH}^+, \text{MCHene}^+/\text{Tetra}^-)$ , and  $\Delta\text{T}^- = \text{ID}_1 - \text{ID}_2$  are shown in Figure 7. They are all dominated by the spectrum of  $\text{Tetra}^-$  ( $\lambda_{\text{max}} = 450 \text{ nm}$ ). The intercept IA should correspond to the sum of the  $\text{M}^{+*}$  and  $\text{Tetra}^-$  free ion yields. Therefore, IA should be larger than  $\Delta\text{T}^-$ . This is clearly not the case. For an explanation, see the Discussion, part B. The rate constants  $k^-$  and  $k_{\text{tot}}$  are independent of  $\lambda$ . The mean values are given in Table 2.

**G.  $\text{N}_2\text{O}$  as Additional Electron Scavenger.** The rate analysis of a  $\text{N}_2\text{O}$  saturated solution of 0.2 M 1112-Tetra (system C, Table 1) confirms the initial observation that the 450 nm band is reduced uniformly by  $\text{N}_2\text{O}$ . The rate constants  $k^-$  and  $k_{\text{tot}}$ , however, remain, within error limits, identical to the results in system A and B (see Table 2). This is proof, that  $e_{\text{solv}}$  is the precursor to the 450 nm band and the band itself must be assigned to  $\text{Tetra}^-$ .  $\text{N}_2\text{O}$  is not affecting  $k_{\text{tot}}$  and therefore further confirms that the  $\text{M}^{+*}$  decay to  $\text{MCH}^+$  and  $\text{MCHene}^+$  is not affected by the solutes such as Tetra and  $\text{N}_2\text{O}$  (Table 2).

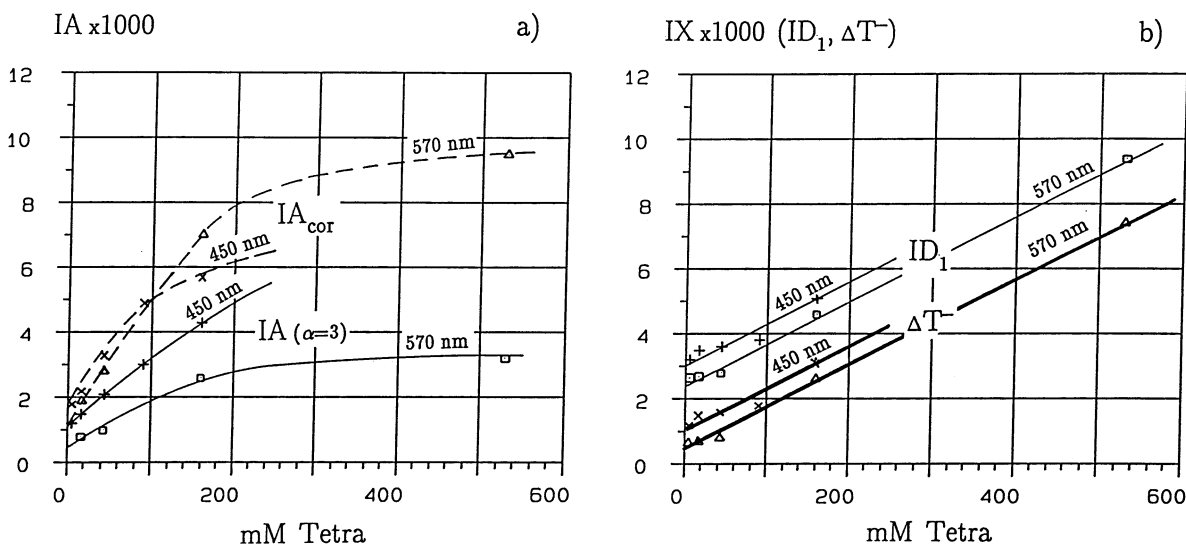


**Figure 6.** Concentration dependence of the free ion intercepts from the chemical system A (Table 1), normalized to 100 Gy. (a)  $IA(M^{++},T^-)$  as determined for  $\alpha = 3.0$  (assumed the mobility for  $M^{++}$  to be identical to that for  $MCH^+$ ).  $IA_{cor}$  (dashed lines), corrected for the higher mobility of  $M^{++}$ :  $\sim 9$  times faster than that of  $MCH^+$  (see Discussion, part B). (b)  $ID_1(MCH^+,MCHene^+/T^-)$  and  $\Delta T^- = ID_1 - ID_{2,calc}$ . The latter represents the  $T^-$  yield in Scheme 1 or the  $T_2^-$  yield in Scheme 2 (see Discussion, part A).

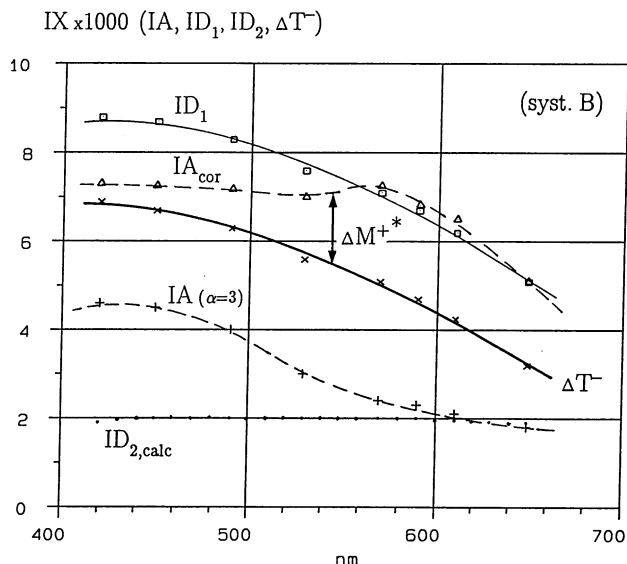


**Figure 7.** Free ion intercept spectra (chemical system B, Table 1), normalized to 100 Gy:  $IA(M^{++}/T^-)$  as determined for  $\alpha = 3.0$  (same mobility as that of  $MCH^+$ ),  $ID_1(MCH^+,MCHene^+/T^-)$ ,  $ID_{2,calc}(MCH^+,MCHene^+/Cl^-)$ , and  $\Delta T^- = ID_1 - ID_2$ .  $IA_{cor}$  is a corrected  $IA$  for the higher mobility of  $M^{++}$  to ascertain that  $IA_{cor} = \Delta T^- + \Delta M^{++}$ .  $\Delta M^{++}$  is the free ion contribution of  $M^{++}$  (for details see Discussion, part B).

The free ion yield of Tetra<sup>-</sup> ( $\Delta T^- = ID_1 - ID_2$ ) is reduced with  $N_2O$  by  $24 \pm 3\%$  (comparison of  $\Delta T^-$  for systems B and C in Figure 8). This is again support for  $e_{solv}$  being the precursor to the 450 nm band (assigned to Tetra<sup>-</sup>).

The initial  $IA(M^{++}/T^-)$  for  $\alpha = 3.0$  (143 K) is again smaller than  $\Delta T^-$ , a discrepancy which will be treated in the Discussion, part B.

**H. Temperature Dependence of the Kinetic Parameters.** The effect was studied for both Tetra isomers at 450 nm: system D for 1112-Tetra and system G for 1122-Tetra (Table 1). The mobility values  $\alpha$  (for  $MCH^+$ ) and  $\delta_{mix}$  (for  $MCH^+$ ,  $MCHene^+$ ), used for the kinetic analysis, are listed in Table 4. From the rate curve simulations, the temperature dependences of  $k^-$  and  $k_{tot}$ , as well as of the intercepts  $IA$ ,  $ID_1$ , and  $\Delta T^- = ID_1 - ID_2$  were derived.

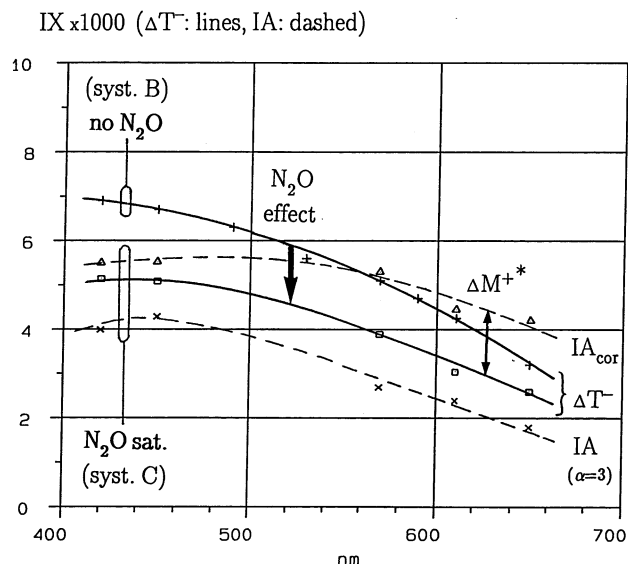


**Figure 8.** Effect of  $N_2O$  on the free ion intercept spectra (chemical system C versus system B, Table 1), particularly on  $\Delta T^- = ID_1 - ID_2$ .  $\Delta T^-$  is reduced by  $24 \pm 3\%$ . For  $IA$  ( $\alpha = 3$ ) and  $IA_{cor}$ , see the caption of Figure 7 and the Discussion, part B.

The Arrhenius plots for the rate constants are shown in Figure 9, and the corresponding data are summarized in Table 3. For  $k^-$  above  $\sim 163$  K there is a beginning deviation from linearity. The attached anion equilibrium (eq 12) is so fast that it is not expected to be the origin of the deviation (see the Discussion, part A).  $\log A$  for the anion decay is about 11. This again excludes the possibility that the 450 nm band would be due to a solvent separated ion pair as for  $CCl_4^{2,15}$  or hexachloroethane<sup>1</sup> in MCH. Its decay would ask for  $\log A$  to be about 9–10.<sup>15,16</sup>

It is surprising that the free ion yield of Tetra<sup>-</sup>, derived from  $\Delta T^- = ID_1 - ID_2$ , is extremely temperature dependent for both isomers (Table 4). The  $G_{fi}$  values vary by a factor of 2 only from 133 to 295 K (162 K difference),<sup>3</sup> whereas  $\Delta T^-$  for 1112-Tetra varies by a factor of 8 over just 30 K (133 to 163 K). This needs an explanation: see the Discussion, part A.

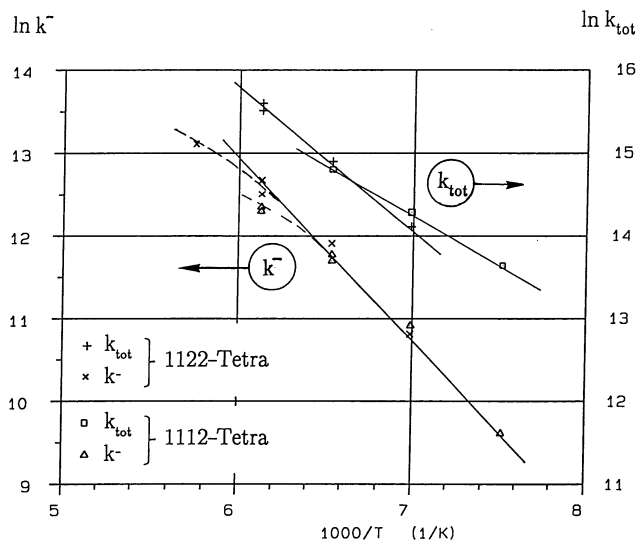


**Figure 9.** Arrhenius plots for the rate constants  $k^-$  and  $k_{\text{tot}}$  for the two isomers 1112-Tetra and 1122-Tetra (chemical systems D and G, Table 1). For the Arrhenius parameters see Table 3.

**TABLE 3: Arrhenius Parameters for the Rate Data ( $\delta_{\text{mix}}$  Model)**

temp range	1112-Tetra (syst D)	1122-Tetra (syst G)
	133–153 K	143–163 K
$k^-$	$E_{\text{act}} = 17.8$ kJ/mol $\log A = 11.19$ $r = 0.9966$	$E_{\text{act}} = 16.9$ kJ/mol $\log A = 10.9$ $r = 0.9915$
$k_{\text{tot}}$	$E_{\text{act}} = 9.83$ kJ/mol $\log A = 9.79$ $r = 0.99994$	$E_{\text{act}} = 13.9$ kJ/mol $\log A = 11.2$ $r = 0.9983$

**TABLE 4: Temperature Dependence of the Mobility Values  $\alpha$  and  $\delta_{\text{mix}}$  as Used in Simulation and of the Experimental “Free Ion Yields”  $\Delta T^-$  at 450 nm**

temp K	$\alpha^a$ at all $\lambda$ $\mu\text{s}^{0.6}$	$\delta_{\text{mix}}^b$ at 450 nm $\mu\text{s}^{0.6}$	$\Delta T^- \times 10^3$ (from $\text{ID}_1 - \text{ID}_2$ )	
			1112-Tetra (syst D)	1122-Tetra (syst G)
133	4.5	7.5	8.2	
143	3.0	5.0 $\diamond$	4.0	11.2
153	2.0	3.3	2.8	8.5
163	1.5	2.5	1.1	5.9
173	1.14	1.9		4.0
183	0.88	1.5		2.6

<sup>a</sup> The mobility value for  $\text{MCH}^+$ .<sup>8</sup> <sup>b</sup>  $\delta_{\text{mix}}$  assumed to be proportional to  $\alpha$  with  $\diamond$  as the experimental reference value ( $\alpha$  is a relevant guideline, since the  $\text{MCH}^+$  yield is about 87%).

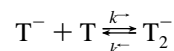
## V. Discussion

**A. Concentration Dependence of the Free Ion Intercepts: The Anion Equilibrium  $\text{T}^- + \text{T} \rightleftharpoons \text{T}_2^-$ .** The intercepts are the sum of the free ion absorptions: for IA from  $\text{M}^{++}$  and  $\text{T}^-$ , for  $\text{ID}_1$  from the mixed cations  $\text{MCH}^+/\text{MCHene}^+$  and  $\text{T}^-$ , and for  $\Delta T^- = \text{ID}_1 - \text{ID}_2$  from  $\text{T}^-$  alone. In all intercepts (except  $\text{ID}_2$ ),  $\text{T}^-$  is involved.

To ensure that the free ion yield of  $\text{T}^-$  is constant, scavenging of  $\text{e}_{\text{solv}}^-$  by  $\text{T}$  must be completed, before the free ion recombination sets in. At 143 K this is at  $t^{-0.6} \approx 0.15 \mu\text{s}^{-0.6}$ .<sup>3</sup> Therefore, the anchor point AP (ref 14) for  $\text{e}_{\text{solv}}^- + \text{T}$  must be higher than  $0.15 \mu\text{s}^{-0.6}$ . With  $k_c = 4.8 \times 10^8 \text{ M}^{-1} \text{ s}^{-1}$  (see Results), this condition means  $[\text{T}] > 0.5 \text{ mM}$ . As our lowest concentration of  $\text{T}$  is 10 times higher, all free ion intercepts should be constant throughout the complete  $[\text{T}]$  range. This is clearly not the case (Figure 6) and is beyond experimental error limits.

Theoretically, such an increase of intercepts with  $[\text{T}]$  could be explained by referring to an ion recombination leading to a product absorber. Equation 10 in ref 1 shows that in this case the intercept depends on  $G_{\text{tot}}$  (total scavenging yield), which obviously is dependent on the scavenger concentration  $[\text{T}]$ . However, it has previously been shown<sup>1</sup> that such a model with large intercepts is not able to simulate the rate curves from the Tetra system.

It remains to consider the formation of dimer anions  $\text{T}_2^-$  through an equilibrium



with  $\text{T}_2^-$  being the absorber at 450 nm (not  $\text{T}^-$ ). With increased  $[\text{T}]$  the equilibrium will be shifted toward  $\text{T}_2^-$  and the corresponding intercept (now due to  $\text{T}_2^-$ ) will increase, in agreement with the experiment (Figure 6).

The kinetics introduced by such an equilibrium is represented by Scheme 2 (Scheme 1 modified for the anion mechanism). The buildup rate for this first-order system is  $k_{\text{up}} = k^-[\text{T}] + k^-$ . So far only electron scavenging had to be completed for the anionic buildup. Now, further delay for the 450 nm absorber ( $\text{T}_2^-$ ) occurs through  $k_{\text{up}}$ . For this purpose the rate constants  $k^-$  and  $k^-$  must be evaluated.

The forward rate constant  $k^-$  is calculated from the diffusion constants  $D(\text{Tetra}) \approx D(\text{Tetra}^-) \approx 10^{-8} \text{ cm}^2 \text{ s}^{-1}$  (see Results). With reactant radii of 0.3 nm, this leads to  $k^-(143 \text{ K}) = 10^7 \text{ M}^{-1} \text{ s}^{-1}$ .

The backward rate constant  $k^-$  is less obvious. It may be estimated from three conditions it has to meet, not to interfere with the experimental findings:

(a) The equilibrium buildup (being  $[\text{T}]$  dependent) should not interfere with the time range in which  $k^-$  is determined, as  $k^-$  is not  $[\text{T}]$  dependent. This means that  $\text{AP}_{\text{up}}$  (the anchor point<sup>14</sup> for the buildup process) should be higher than the starting point for  $k^-$  matching:  $\text{AP}_{\text{up}} > 0.7$ . This means  $k_{\text{up}} > 2.5 \times 10^6 \text{ s}^{-1}$ , and  $k^- > 2.4 \times 10^6 \text{ s}^{-1}$  from the lowest  $[\text{T}]$ .

(b) Similarly,  $k_{\text{tot}}$  is independent of  $[\text{T}]$  for  $[\text{T}] \geq 50 \text{ mM}$  and should therefore not be disturbed by  $k_{\text{up}}$  in the range  $\text{AP}_{\text{tot}} < t^{-0.6} \leq \text{AP}_{\text{tot}} + 0.6$ , the range which is needed for the  $k_{\text{tot}}$  determination. With  $\text{AP}_{\text{tot}} = 0.53$  the condition is  $\text{AP}_{\text{up}} > 1.2$ . This means  $k_{\text{up}} > 6.2 \times 10^6 \text{ s}^{-1}$ , and  $k^- > 5.7 \times 10^6 \text{ s}^{-1}$  for 50 mM Tetra.

(c) Simulation in the early stage ( $1.2 < t^{-0.6} < 4 \mu\text{s}^{-0.6}$ ) defines the intercept IA for  $\alpha = 3$ . If the equilibrium buildup (with  $\text{AP}_{\text{up}}$ ) would reach into this  $t^{-0.6}$  range, the rate curve would further deviate toward earlier times and a single parameter IA would not be able to simulate the early stage. The condition for this early stage therefore is  $\text{AP}_{\text{up}}(10\%) \geq 3.0 \mu\text{s}^{-0.6}$  (ref 14) (10% rest of buildup reaction due to larger noise level in this early time). This yields  $k_{\text{up}} > 1.5 \times 10^7 \text{ s}^{-1}$  and therefore  $k^- \geq 1.5 \times 10^7 \text{ s}^{-1}$  for the lowest  $[\text{T}]$ .

Condition c obviously is the most stringent one. In fact, the equilibration is very fast:  $\tau_{\text{up}} < 66 \text{ ns}$ . It is therefore not possible to distinguish whether fragmentation occurs from the monomer or dimer anion, from  $\text{T}^-$  or  $\text{T}_2^-$ , or from both. The equilibrium rate data also reveal that the  $\text{T}_2^-$  yield is less than half of the total free ion yield (for the  $[\text{T}]$  range studied: chemical system A). This finds support in Figure 6b, where  $\Delta T^-$  ( $\text{T}_2^-$  yield) is about linear up to 530 mM Tetra (not yet leveling off).

It is concluded that Scheme 2 with the equilibrium  $\text{T}^- + \text{T} \rightleftharpoons \text{T}_2^-$  is able to reproduce the facts. This also explains the strong temperature dependence of  $\Delta T^- = \text{ID}_1 - \text{ID}_2$  (Table 4),

as  $\Delta T^-$  now is due to  $T_2^-$  and the temperature effect is through the equilibrium. It is expected that the absorption band for  $T_2^-$  at 450 nm corresponds to a charge resonance band ( $T \leftarrow T^-$ ). The relatively large bandwidth (Figure 1) might be support for that assignment.

**B. Precursor  $M^{+*}$  and Its Mobility.** In Figure 7 the intercept spectrum for IA ( $\alpha=3$ ), due to the free ion yields of  $M^{+*}$  and  $T^-$ , was found to be smaller than  $\Delta T^-$  for  $T^-$  alone ( $T^-$  now should be replaced by  $T_2^-$ ; see previous paragraph). IA has to be larger than  $\Delta T^-$  by the free ion contribution of  $M^{+*}$  (here called  $\Delta M^{+*}$ ). One should remember that, originally,<sup>9</sup> the mobility of  $M^{+*}$ , with a lack of any criteria, was assumed to be identical to the mobility of  $MCH^+$ :  $\alpha(M^{+*}) = \alpha(MCH^+) = 3.0 \mu s^{0.6}$  at 143 K. This allowed us to derive an absolute spectrum  $\epsilon(M^{+*})$  from the intercept spectrum of  $M^{+*}$ .<sup>9</sup> These  $\epsilon(M^{+*})$  values now appear to be too low. To increase IA to a value larger than  $\Delta T^-$ , the  $\alpha$  value must be lowered, which means the mobility of  $M^{+*}$  must be higher than that for  $MCH^+$ .

*The amount of lowering  $\alpha$  was determined by the following iteration:* The initial IA was set to  $IA_1 = \Delta T_{exp}^- + \Delta M^{+*}$  (from ref 9 with  $\alpha_0 = 3.0$ ). With this new IA, a new, lower  $\alpha$  had to be derived by simulation of the experimental rate curve at early times ( $2 \leq t^{-0.6} \leq 4 \mu s^{-0.6}$ ). The new  $\alpha$  initiates a higher contribution of  $\Delta M^{+*}$ .<sup>9</sup> For the  $i$  step of the iteration,  $IA_i = \Delta T_{exp}^- + \Delta M^{+*}(\alpha_{i-1})$  and the simulation again yields a new  $\alpha_i$ . The iteration ends when  $\alpha_i$  does not alter any more.

*The final  $\alpha$  is called  $\alpha_{cor}$ . The corrected intercepts  $IA_{cor}$  are shown in Figure 7 and in Figure 6a. The area in Figure 7 between  $IA_{cor}$  and  $\Delta T^-$  corresponds to the final  $\Delta M^{+*}$  contribution. Unexpectedly, the values for  $\alpha_{cor}$  systematically vary with  $\lambda$  with a maximum at 450 nm ( $\alpha_{cor} = 1.7$ ) and a minimum around 600 nm ( $\alpha_{cor} = 0.8$ ). As the effect is systematic, quoting an average value is not reasonable. From a detailed search for the origin of this puzzling  $\lambda$  dependence, it became rather firm that the difficulty relates to the accuracy with which  $\Delta T^-$  was determined from the intercept differences ( $ID_1 - ID_2$ ). In the range  $570 < \lambda < 650$  nm the values for  $\alpha_{cor}$  are almost independent, whether  $\Delta T^- = ID_1 - ID_2$  values were determined with  $\delta_{mix}$  or  $\delta_{fast}$  (see the Discussion, part C). It is concluded that the data in this  $\lambda$  range are more reliable:  $\overline{\alpha_{cor}} = 0.83 \pm 0.05 \mu s^{0.6}$ . Due to eq 1 the corresponding  $M^{+*}$  mobility,  $D(M^{+*})$ , is about 9 times higher than that for  $MCH^+$ . The  $M^{+*}$  free ion spectrum ( $\epsilon(M^{+*})$ ) must be about 3 times larger than that previously published.<sup>9</sup>*

*Due to the anion equilibrium  $T^- + T \rightleftharpoons T_2^-$  introduced in the previous paragraph, the experimental  $\Delta T^-$  value ( $T_2^-$  absorption) does not represent the total free anion yield. With a correction to 100% anion yield,  $\alpha_{cor}$  would be even lower and the mobility of  $M^{+*}$  higher than 9 times the mobility of  $MCH^+$ , and  $\epsilon(M^{+*})$  would increase by more than 3 times over the published value.<sup>9</sup> Due to these unknown corrections, one should not derive absolute values for  $D(M^{+*})$  and  $\epsilon(M^{+*})$ .*

*For the  $N_2O$  saturated 0.2 M Tetra solution (chemical system C), Figure 8 shows again that IA is smaller than  $\Delta T^-$  and therefore again needs a correction to higher mobility of  $M^{+*}$  with a lower  $\alpha_{cor}$ . The corrected  $IA_{cor}$  is shown in Figure 8. From the  $\lambda$  range 570–650 nm,  $\overline{\alpha_{cor}} = 1.32 \pm 0.19$  is higher than that for the system without  $N_2O$ . This reflects the fact that  $\Delta T^-$  ( $T_2^-$  absorption) not only is lower due to the anion equilibrium,  $T^- + T \rightleftharpoons T_2^-$ , but also is due to  $N_2O$  scavenging (by  $-24\%$ ). These results from system C are quite compatible with the proposal of higher mobility for  $M^{+*}$ .*

Previously, the effect of  $N_2O$  (ref 9) or  $CHCl_3$  (ref 8) was compared with a quenching effect on  $M^{+*}$ , as the solute affected the yield of relaxed  $MCH^+$  relative to the fragment cation  $MCHene^+$ . In the  $MCH$  solution of Tetra, this is not the case (no  $[T]$  dependence of  $k_{tot}$ ). This indicates that the star (\*) in  $M^{+*}$  rather signals a state of higher energy (or of higher ionization potential), in agreement with the conclusions in the paper on quadricyclane in  $MCH$ .<sup>11</sup>

**C. Comment.** It has been suggested that the model with  $\delta_{mix}$  (mixed cation pair with 13%  $MCHene^+$  and 87%  $MCH^+$ ) is more likely than the model with  $\delta_{fast}$  ( $MCH^+$  as the only product cation). In this paper all results therefore are given for  $\delta_{mix}$  (Figure 4). However, it cannot be excluded that the real  $\delta$  value is somewhere between  $\delta_{mix}$  and  $\delta_{fast}$ . This comment summarizes the effect on the results, if, in the extreme case,  $\delta_{real} = \delta_{fast}$ .

*The anion lifetime ( $k^-$ ) would not change. The rate constant  $k_{tot}$  is about 10% larger but still not dependent on  $[T]$  ( $k_2 = 0$ ). The Arrhenius plots for  $k^-$  and  $k_{tot}$  for both isomers are parallel and very close to the curves in Figure 9. For  $k^-$ ,  $E_{act}$  is smaller by 4–10% and  $\log A$  by 2–6%. For  $k_{tot}$ ,  $E_{act}$  is smaller by 4–14% and  $\log A$  by 1–4% (first number is for 1122-Tetra, second for 1112-Tetra). The intercepts  $ID_1$  ( $MCH^+/T_2^-$ ) and  $\Delta T^-$  (yield of  $T_2^-$ ) are about two times larger (because  $\delta$  is lower) with the same concentration dependence as those in Figures 6b, 7, and 8. The derived  $\alpha_{cor}$  values (see the Discussion, part B) are about 17% lower, which means that the stated mobility minimum for  $M^{+*}$  would be about 36% larger (means at least 12 times the mobility of  $MCH^+$ ). The conclusion in the previous paragraph (Discussion, part B) remains valid: the  $M^{+*}$  mobility is at least 9 times higher than the one for  $MCH^+$ .*

**Acknowledgment.** Support by the Swiss National Science Foundation and by the Research Funds of the ETH-Zürich is gratefully acknowledged.

## References and Notes

- Quadir, M. A.; Azuma, T.; Domazou, A. S.; Katsumura, Y.; Bühler, R. E. *J. Phys. Chem. A* **2003**, *107*, 11361.
- Bühler, R. E. *Radiat. Phys. Chem.* **2001**, *60*, 323.
- Katsumura, Y.; Azuma, T.; Quadir, M. A.; Domazou, A. S.; Bühler, R. E. *J. Phys. Chem.* **1995**, *99*, 12814.
- Hurni, B.; Brühlmann, U.; Bühler, R. E. *Radiat. Phys. Chem.* **1975**, *7*, 499.
- van den Ende, C. A. M.; Warman, J.; Hummel, A. *Radiat. Phys. Chem.* **1984**, *23*, 55.
- Bartczak, W. M.; Hummel, A. *Radiat. Phys. Chem.* **1994**, *44*, 335.
- Bartczak, W. M.; Hummel, A. *Radiat. Phys. Chem.* **1997**, *49*, 675.
- Bühler, R. E.; Domazou, A. S.; Katsumura, Y. *J. Phys. Chem. A* **1999**, *103*, 4986.
- Bühler, R. E.; Katsumura, Y. *J. Phys. Chem.* **1998**, *102*, 111.
- Bühler, R. E. *Can. J. Phys.* **1990**, *68*, 918.
- Bühler, R. E.; Quadir, M. A. *J. Phys. Chem. A* **2000**, *104*, 2634.
- Bühler, R. E. *Proc. Trombay Symposium on Radiation and Photochemistry TSRP 98*, BARC, Trombay, Mumbai, India, Jan 14–19, 1998; part II, p 429.
- Bühler, R. E. *Res. Chem. Intermed.* **1999**, *25*, 259. Due to printing errors, ask the author for a corrected reprint.
- Due to time compression toward late times in  $t^{-0.6}$  plots, the “end” of a reaction corresponds to an easily recognizable point, called the “anchor point” (AP) for the particular reaction.<sup>13</sup> It is usually calculated for 99% completion of the reaction (1% rest) by  $AP = x(k_1 \times 10^{-6})^{0.6} \mu s^{-0.6}$  with  $x = 0.4$ . For 5% rest, AP(5%) has  $x \approx 0.5$ , and for 10% rest, AP(10%) has  $x \approx 0.6$ .
- Gebicki, J. L.; Domazou, A. S.; Ha, T.-K.; Cirelli, G.; Bühler, R. E. *J. Phys. Chem.* **1994**, *98*, 9570.
- Domazou, A. S.; Quadir, M. A.; Bühler, R. E. *J. Phys. Chem.* **1994**, *98*, 2877.